Fractal Dimension in Human Cerebellum Measured by Magnetic Resonance Imaging

Jing Z. Liu,*† Lu D. Zhang,*‡ and Guang H. Yue*‡
*Department of Biomedical Engineering, The Lerner Research Institute, The Cleveland Clinic Foundation, Cleveland, Ohio; and Departments of †Physics and ‡Biomedical Engineering, Case Western Reserve University, Cleveland, Ohio

ABSTRACT Fractal dimension has been used to quantify the structures of a wide range of objects in biology and medicine. We measured fractal dimension of human cerebellum (CB) in magnetic resonance images of 24 healthy young subjects (12 men and 12 women). CB images were resampled to a series of image sets with different 3D resolutions. At each resolution, the skeleton of the CB white matter was obtained and the number of pixels belonging to the skeleton was determined. Fractal dimension of the CB skeleton was calculated using the box-counting method. The results indicated that the CB skeleton is a highly fractal structure, with a fractal dimension of 2.57 ± 0.01. No significant difference in the CB fractal dimension was observed between men and women.

INTRODUCTION

Fractal, first introduced by Mandelbrot (1982), is a concept to characterize spatial or temporal phenomena that are continuous but not differentiable. Mathematically, a fractal structure is defined as a set that has a fractal dimension (FD) exceeding its topological one. Unlike the more familiar Euclidean structures, magnifying a fractal results in the resolution of more details. Fractal objects are everywhere in nature, such as coastlines, clouds, trees, and snowflakes. Fractal properties include self-similarity, scale invariance, infinite amount of details, etc. Fractal analysis provides a useful tool to quantify the inherent irregularity of a fractal object by a number, i.e., FD, which is usually a fractional value. FD serves as an index of the morphometric complexity and variability of the object being studied.

Fractal analysis has recently been applied to study a wide range of objects in biology and medicine (Kenkel and Walker, 1996; Cross, 1997; Heymans et al., 2000; Losa, 2000), especially in brain structures and processes. It has been used successfully in quantifying brain cell morphologies (Porter et al., 1991; Smith et al., 1991, 1993; Takeda et al., 1992; Smith and Behar, 1994; Soltys et al., 2001) and the shape of the brain (Bullmore et al., 1994; Cook et al., 1995; Free et al., 1996; Thompson et al., 1996; Rybaczuk et al., 1996; Rybaczuk and Kedzia, 1996; Kedzia et al., 1997, 2002; Pereira et al., 2000; Iftekharuddin et al., 2000; Blanton et al., 2001). Bullmore et al. (1994) measured the complexity of the boundaries between the white matter (WM) and gray matter (GM) in human brain magnetic resonance (MR) images and applied the results to a controlled study of schizophrenic and manic-depressive patients. They determined the mean FD of all subjects to be 1.402, and found that the manic-depressive patients had higher FD than controls, whereas the schizophrenic patients had lower FD than controls. Thompson et al. (1996) quantified morphometric variance of the surfaces of the supracallosal sulcus, the cingulate and marginal sulci, the anterior and posterior rami of the calcarine sulcus, and the parietooccipital sulcus in cryoplaned specimen photographs of human brain, and found that the FDs of these structures were in a narrow range around 2.10. The investigators concluded, based on their observation of low variance in the FD, that there was a stable FD value for normal brain, which could be used as a control for pathological studies. Blanton et al. (2001) investigated the influence of age and gender on structural complexity and cortical sulcus developmental trends in children and adolescents by measuring FD of the surface of the brain sulcal/gyral convolution in MR images using the algorithm of Thompson et al. (1996). Their results showed significant age-related FD changes in the frontal regions and gender-related FD alterations in the left superior frontal and right inferior frontal regions. Free et al. (1996) studied the convolution of cerebral cortex by measuring variance in the WM surface in human brain MR images, and obtained the FD in a narrow range from 2.24 to 2.41. The investigators found a high degree of symmetry in FD between the right and left hemispheres in the subjects aged from 23 to 53, whereas no gender-related difference was observed. Differences in FD between the normal gyral patterns and those in epilepsy were compared, and the abnormality expressed by FD in epilepsy was determined. Kedzia et al. (2002) studied the microangioarchitecture of human brain vessels during the fetal period and found that FD increased from 1.26 in the fourth month to 1.53 in the fifth month and 1.6 in the sixth and seventh months. The results showed a close correspondence between structure and function. Pereira et al. (2000) quantified the edge irregularities of brain lesions to evaluate the degree of tumor malignancy in human brain MR images. Iftekharuddin et al. (2000) used FD to

Submitted March 7, 2003, and accepted for publication August 15, 2003.

Address reprint requests to Jing Z. Liu, PhD, Dept. of Biomedical Engineering/ND20, The Cleveland Clinic Foundation, 9500 Euclid Ave., Cleveland, OH 44195 USA. Tel.: 216-445-6735; Fax: 216-444-9198; E-mail: liuj@bme.ri.ccf.org.

0006-3495/03/12/4041/06 $2.00

detect and locate brain tumors. Their method may be applied to extract progressive tumor development information by comparing it to normal brain data. Kedzia et al. (1997) studied senile brain atrophy by comparing the young brain (NMR data) and the older brain with visible senile changes (photo data). They found that the FDs of the gray matter surfaces were 2.35 for the younger brain and 2.29 for the senile brain. Cook et al. (1995) estimated the FD of the cortical WM boundary in MR images of normal human brain and compared it with those of patients with frontal lobe epilepsy, temporal lobe epilepsy, and dementia of Alzheimer type. They concluded that patients with frontal lobe epilepsy had decreased FD (FD $<$ 1.27) whereas patients with temporal lobe epilepsy and dementia had FDs in the normal range (1.32–1.48 and 1.37–1.50, respectively).

Although fractal research on the brain has been ongoing, little work has been done on the human cerebellum (CB). Most studies in the literature were dealing with CB cell morphometrics (Takeda et al., 1992; Smith et al., 1993). Only one group applied FD to evaluate CB surface complexity (Rybaczuk et al., 1996; Rybaczuk and Kedzia, 1996). They quantified the CB growth process by measuring the FD from 120 crown–rump (C–R) length to 200 C–R length in the fetal period (Rybaczuk et al., 1996). They observed that the FD increased to 2.25 from 120 to 130 C-R, decreased to 2.12 from 130 to 180 C-R, then increased to 2.26 from 180 to 200 C-R, resulting from corresponding bulk growth (reducing FD) and surface growth (augmenting FD) at the different developmental stages. The investigators then measured the FD of adult CB surface and compared it to the FD of the fetal CB (Rybaczuk and Kedzia, 1996). They found that the adult FD, which was in the range of 2.25–2.30, slightly exceeded the FD of fetal CB at the final growth period.

Despite the fact that the skeleton is a very important morphometric character of an image, there has been no report on the fractal property of the skeleton of human CB WM. As is apparent from the MR CB images, the CB WM bears a tree-like pattern, which resembles a fractal structure. The purpose of this study was to measure the FD of human CB skeleton using T_1-weighted MR head images. Since the shape of CB WM is well represented by its skeleton, it is expected that morphometric changes in CB WM due to WM diseases may be evaluated using the WM skeleton. Moreover, interior CB lesions may be studied by skeleton, whereas CB surface evaluation in the previous studies can only be used to examine lesions on the surface. Therefore, it is desirable to develop a method to extract the CB WM skeleton and explore its usefulness in analyzing FD of CB. In this study, the skeleton of human CB WM was first created from the MR CB images at different spatial resolutions, and the FD was then calculated by applying the box-counting definition. The significance and potential applications of the FD are addressed and possible improvements of the method are suggested in Discussion.

MATERIALS AND METHODS

Subjects

Twenty-four young healthy subjects (17–35 years old, mean age $\pm$ SD = 27.7 $\pm$ 4.4) participated in the study, including 12 men (20–35 years old, mean age $\pm$ SD = 28.8 $\pm$ 3.7) and 12 women (17–35 years old, mean age $\pm$ SD = 26.7 $\pm$ 5.0). The experimental procedures were approved by the Institutional Review Board at the Cleveland Clinic Foundation. All subjects signed informed consent before participating.

Collection of MR head images

Coronal MR brain images covering the whole cerebellum were collected on a 1.5-T Siemens Vision scanner (Erlangen, Germany) using a circularly polarized head coil. A total of 128 contiguous coronal brain slices (each 2 mm thick) were imaged with the 3D Turboflash imaging sequence (TR (repetition time)/TE (echo time) = 11.4/4.4 ms). The flip angle was 10° and the in-plane resolution was 1×1 mm^2.

Segmentation and resampling of CB images

The CB images were segmented out manually from the collected head images. Background noise in each slice was removed by deleting the pixels with intensities lower than a certain threshold. The images were then standardized to the same dimension (matrix size = 128×64, pixel size = 1×1 mm^2, slice thickness = 2 mm). The number of CB slices was 23–29, depending on the individual subject. The segmented CB images were resampled to be 1 mm in thickness to keep the isotropy (Fig. 1).

The resultant images were further resampled to a series of image sets with different 3D resolutions (Δ), i.e., 1/4, 1/2, 2, and 4 mm (Fig. 1). The resampling was performed using the subvoxel interpolation algorithm, i.e., the so-called point spread function (PSF) resampling, in the MEDx 3.2 software (Sensor Systems, Sterling, VA). The algorithm considered each image value as a weighted integral, and the weighting function was the PSF

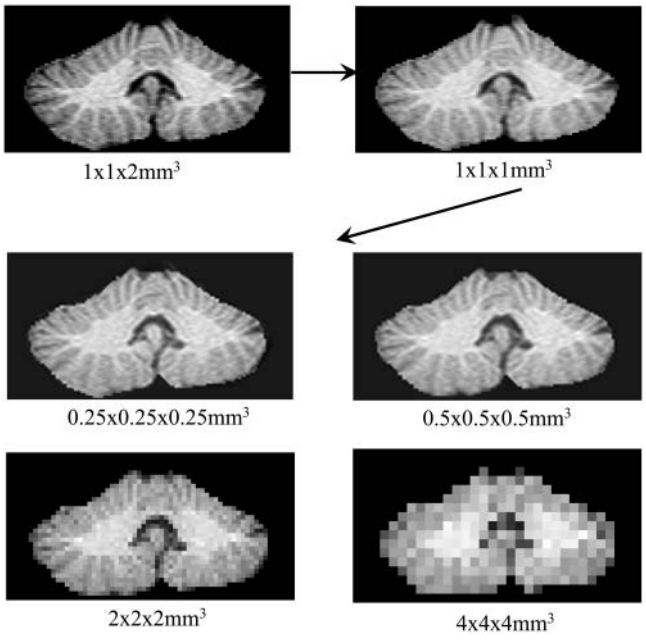

FIGURE 1 A sample slice of CB MR image and its resampling to different resolutions. The spatial resolution (voxel size) is indicated below each image.

of the imaging sensor. The cubic convolution approach, specified in a kernel file, was used to approximate the PSF (Boult and Wolberg, 1993). In most cases, this algorithm provided excellent results compared with the nearest-neighbor or trilinear resampling approaches. All the image analyses were performed on a Sun UltraSPARC (Sun Microsystems, Santa Clara, CA) 333 MHz workstation with 640 MB RAM.

Segmentation of WM and GM

The interfaces between WM and GM in each image set were extracted using a user-modified contour algorithm in Matlab 6.1 (The MathWorks, Natick, MA). The histogram (Fig. 2) was used to determine the threshold between WM and GM. Denoting the intensity of the highest peak (A, corresponding to GM); and the intensity of the valley after the GM peak (B), the threshold was taken as $A + (B - A)/3$. This selection was based on our experience after comparing results obtained using different thresholds. After thresholding, GM was removed, and the contour image of WM was obtained in each slice (Fig. 3 *a*). The rendered contour images were then converted to binary images, i.e., intensities of pixels inside the contours were assigned the value 1, otherwise 0 (Fig. 3 *b*).

Extraction of WM skeleton

The thinning method in the Matlab 6.1 image processing toolbox was applied to the binary images. CB skeletons were obtained from each image slice by iteratively deleting successive layers of pixels on the boundary of WM images until only a skeleton remained (Fig. 3 *c*) (Lam et al., 1992).

The resultant skeletons in each resolution were color-washed and overlaid onto the corresponding CB images so that we could inspect the accuracy of the skeleton extraction method (Figs. 3 *d* and 4).

Measurement of CB fractal dimension

The box-counting method (Mandelbrot, 1982; Kenkel and Walker, 1996) was adopted to compute the FD (D) of the CB skeleton. This method is suitable for structures that lack strict self-similarity. At each resolution Δ (i.e., 1/4, 1/2, 1, 2, and 4 mm), the number of pixels (N) belonging to the CB skeleton was counted in each slice and then summed over all the CB slices.

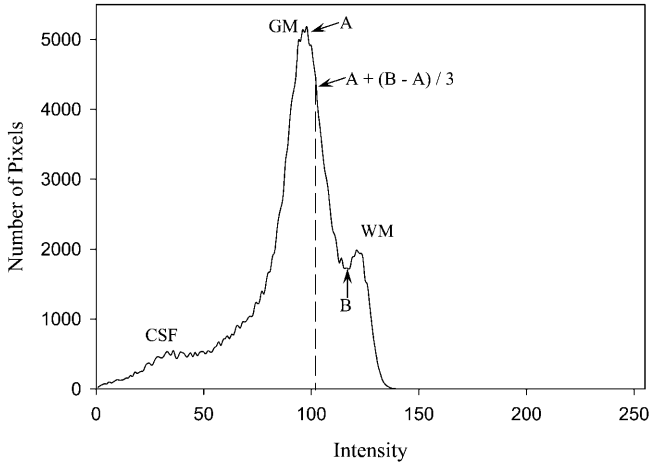

FIGURE 2 Histogram of the CB image set of a subject. The x axis indicates the intensity of the pixels; the y axis indicates the number of pixels at each intensity value. The threshold for separating the white matter (*WM*) and gray matter (*GM*) is indicated by the vertical dashed line between the GM and WM peaks.

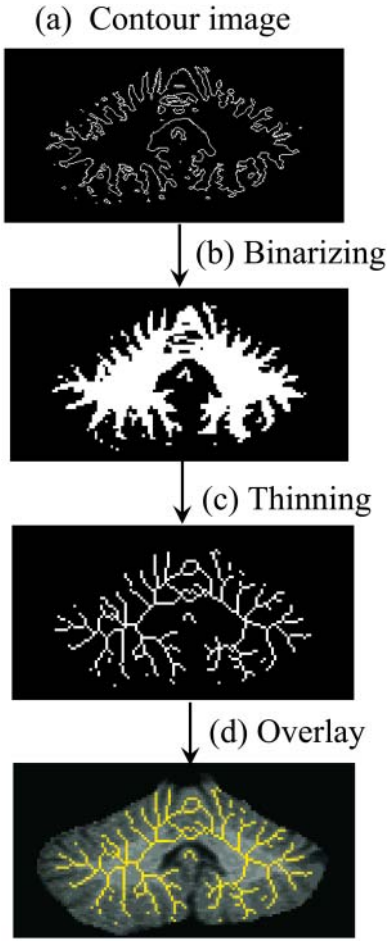

FIGURE 3 Illustration of the steps to extract the CB skeleton in a sample slice. (*a*) A contour image was created by thresholding. (*b*) A binary image was generated by assigning value 1 to the pixels inside the contour. (*c*) The skeleton of the CB image was produced by thinning the binary image. (*d*) The CB skeleton was color-washed and overlaid onto the original CB image.

The counting of the skeleton pixels was performed using the MEDx 3.2 software. The FD is defined in the power-law relationship:

$$N = C\Delta^{-D} \quad (1)$$

where C is a constant. The FD (D) was obtained by linearly fitting $\ln(N) = \ln(C) - D\ln(\Delta)$ (Fig. 5).

Statistical analysis

The FDs of the men and women groups were compared using the independent t-test (at 95% confidence level) to determine if significant difference existed between genders.

RESULTS

In Fig. 4, two sample slices of the CB from two subjects in different resolutions are shown. In each subject, the images became more blurred from the top images to the bottom ones due to reduced spatial resolution. The extracted WM skeletons, being overlaid onto the original CB images, are

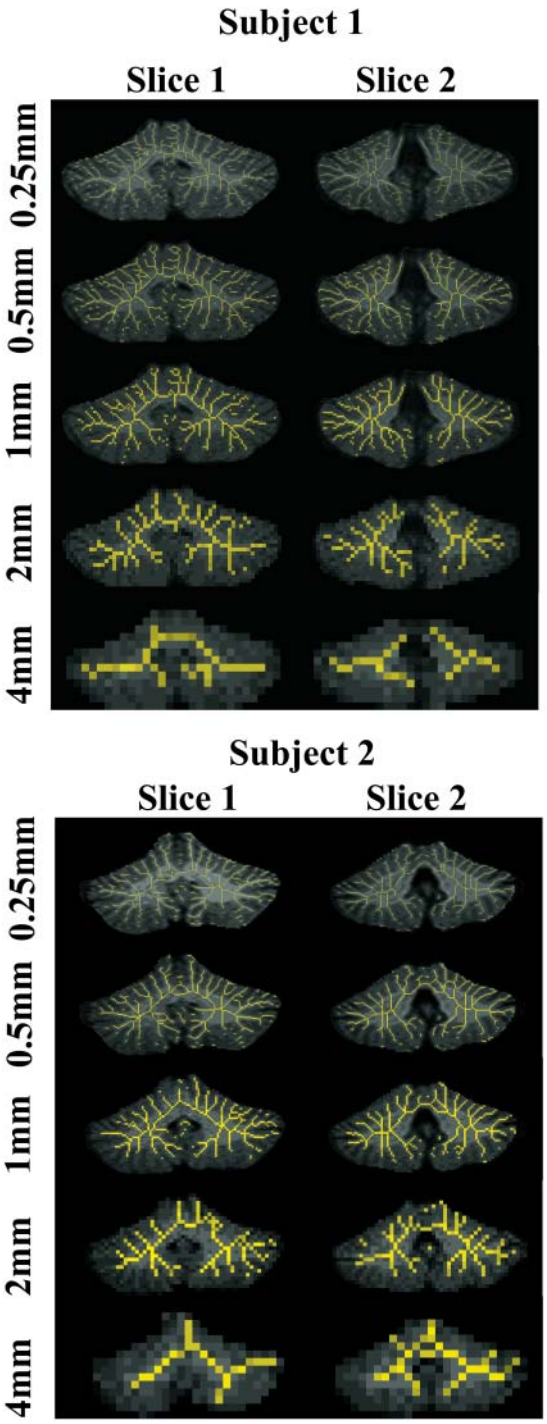

FIGURE 4 Illustration of the generated CB skeletons in two sample slices from two subjects. The skeletons were overlaid onto the original CB images in different resolutions. Visual inspection showed that skeletons of the CB WM were reproduced with reasonable accuracy.

in yellow color. These images show that WM skeletons were generated at satisfactory accuracy using the methods described previously.

The computed FDs for the 24 subjects are listed in Table 1. The FDs were 2.571 ± 0.006 and 2.569 ± 0.007 (mean ± SE of the mean (SEM)) for the men and women groups, respectively. No significant difference was detected between genders by the independent t-test at 95% confidence level in our examined age range ($t = 0.28$, $P = 0.78$). The correlation coefficients (R^2) of the regression fits are also listed in Table 1, which show that the data were fitted by linear functions excellently ($R^2 = 0.9949 \pm 0.0002$ for men, $R^2 = 0.9946 \pm 0.0002$ for women).

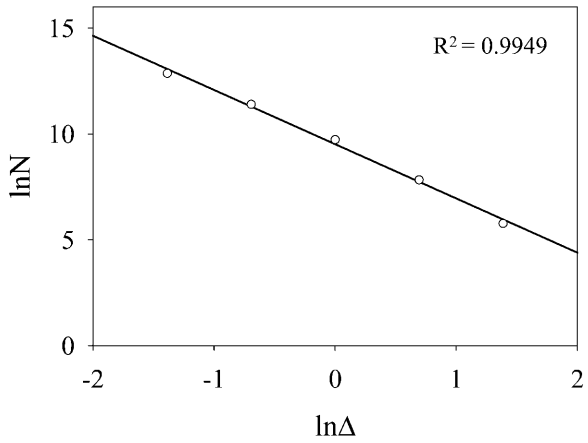

FIGURE 5 Illustration of the linear fit to obtain the fractal dimension in a single subject. The x axis is image resolution (Δ) and the y axis is number of pixels in the skeleton (N) in logarithmic scale. The data (*open circles*) were fitted using linear regression. The negative slope of the fitted curve (*solid line*) represents the fractal dimension. The figure and the high correlation coefficient (R^2) show that the data can be fitted by a linear function excellently.

DISCUSSION

We measured the FD of human CB WM skeleton at 2.57 ± 0.01. This indicates that human CB is a highly fractal structure, consistent with conclusions drawn from studies

TABLE 1 Results of fractal dimension (FD) in cerebellum

	Men		Women		R^2	
Subject	Age	FD	Age	FD	Men	Women
1	20	2.540	17	2.557	0.9953	0.9948
2	26	2.547	20	2.578	0.9948	0.9950
3	27	2.596	23	2.562	0.9961	0.9945
4	28	2.563	25	2.622	0.9954	0.9934
5	28	2.591	26	2.562	0.9949	0.9943
6	28	2.583	27	2.562	0.9943	0.9941
7	29	2.580	27	2.558	0.9949	0.9953
8	30	2.587	29	2.581	0.9949	0.9948
9	30	2.589	29	2.541	0.9936	0.9955
10	32	2.541	30	2.551	0.9950	0.9953
11	32	2.564	32	2.584	0.9950	0.9948
12	35	2.576	35	2.568	0.9943	0.9936
Average	28.8	2.571	26.7	2.569	0.9949	0.9946
SE	1.1	0.006	1.4	0.007	0.0002	0.0002

SE is standard error of the mean. R^2 is the correlation coefficient of the linear fit.

of the CB surface (Rybaczuk et al., 1996; Rybaczuk and Kedzia, 1996). Our results are notably higher than those of the former studies as mentioned in the introduction. This is because different structures were evaluated in their and our studies. Most of the other studies measured FDs of the brain or cerebellum surfaces/boundaries whereas we measured that of the CB WM skeleton. Therefore, it is not strange to see the differences between their results and our results because different structures are expected, in general, to have different FD values. Meanwhile, the differences between the FDs evaluated from different aspects of the same structure (e.g., surface, boundary, and skeleton of the CB) suggest that a single structure may bear different FDs depending on the angles of view. Therefore, it may be necessary to evaluate the fractal properties of a biological structure, especially those of high complexity such as the brain and CB, from different aspects to make a more comprehensive understanding.

The FDs in our study were in a small range (2.540–2.596) and did not change significantly with age (17–35 years), which is consistent with the studies on cerebrum sulcal surface (Thompson et al., 1996) and white-matter surface (Free et al., 1996). However, the FD of the CB changes significantly during the fetal period, as demonstrated by Rybaczuk et al. (1996). Age-related changes in FD of sulcal surface in frontal regions of the cerebrum were also found in children and adolescents (Blanton et al., 2001). For the elderly people, decreases in brain gray matter surface FD were observed (Kedzia et al., 1997). These findings seem to suggest that the FD of human brain may be relatively invariable in some specific age ranges. Once developed, the human brain and its FD may remain relatively stable for a certain period of time. Furthermore, FD changes of the brain with age may not be in a progressive and continuous pattern but may occur abruptly at some particular age ranges. It is also possible that significant changes may be found in certain specific areas of the brain while the global FD of the whole brain remains relatively constant.

We found no significant difference between the FDs of the men and women, which is consistent with the observation by Free et al. (1996). However, a recent study reported gender-related differences when quantifying specific regions of the cerebrum (Blanton et al., 2001). These findings may suggest that there are no gender-related differences in FD of the whole brain in men and women of the same age range, even though differences may indeed exist in certain localized regions. Based on the present data, the same may hold true not only for the brain, but also for the CB.

Another important aspect is regarding the comparison of FD between patients and normal individuals. As suggested by previous studies, some patients may have FDs similar to those of normal subjects, especially when the brain was quantified as a whole (Cook et al., 1995; Free et al., 1996). For example, Cook and his co-investigators (1995) found no differences in the FDs of the cortical WM boundary between normal subjects and patients with temporal lobe epilepsy and dementia (whereas patients with frontal lobe epilepsy did have lower FD). These findings suggest that either the tested patients had no structural degeneration in the measured cortical regions or the FD measure is not sensitive enough to identify adaptive changes in these particular patient populations. The sensitivity may be improved by quantifying FD separately in specific cortical or CB regions, such as the cerebrocerebellum, spinocerebellum, and vestibulocerebellum (Ghez and Thach, 2000), especially when the quantified regions suffered damage or pathological changes. It is reasonable to expect that structural changes after brain or CB damage may lead to detectable FD changes, as also suggested in the previous studies (Bullmore et al., 1994; Cook et al., 1995; Free et al., 1996; Pereira et al., 2000; Iftekharuddin et al., 2000). In our view, quantification of brain structures by FD, either in normal or diseased conditions, will be a major application in future FD-related biomedical research.

The accuracy of the skeleton extraction method directly affects the accuracy of the FD computation. The images in Fig. 4 show that the skeleton generated by our method represented the true CB skeletal structure with satisfactory accuracy. However, the generated skeleton was not connected in some areas due to thresholding. This may have little influence on the FD calculation because the box-counting dimension does not require branch connection. The method may need to be improved if other definitions of FD are to be used. In the data aspect, the best way is to collect raw imaging data at different resolutions directly rather than resampling the images. However, this is not practicable at this time for us due to the limit of the MR imaging technique. That's to say, using a 1.5 T MR image scanner, the spatial resolution cannot reach the values required by our image processing method, i.e., $0.25 \times 0.25 \times 0.25$ mm^3 or $0.5 \times 0.5 \times 0.5$ mm^3. If we choose to do it anyway, the image quality will be deteriorated. However, when MR imaging advances (e.g., with higher magnetic field, faster imaging speed, more sensitive signal detection, etc.) in the future, it may become possible to do so and we may consider doing it. Another concern is that the skeleton extraction method used in the study is not a true 3D algorithm. The skeletons were obtained in 2D slices rather than in a 3D environment. This may introduce certain errors to the FD computation due to the lack of information on the connection relationship between the slices. An accurate 3D skeletonization algorithm is certainly useful in improving the accuracy of the FD calculation as well as in other brain studies. Additionally, a quantitative method to validate the skeletonization is also in demand even though there has not been an effective one in the field due to various difficulties. Investigation of the accuracy of the reconstructed CB images from the skeletons would be a good approach and may be explored in the future.

As a final remark, fractal geometry is a useful tool to describe and understand various biological systems with fractal properties. FD may serve as an index for quantifying

structural or functional complexity of the neural system during the stages of development, degeneration, reorganization, or evolution because in these processes the FD may be dynamically changing (Rybaczuk et al., 1996; Rybaczuk and Kedzia, 1996; Kedzia et al., 2002). The method we developed in this project and its future improvements might potentially be applied to study CB or the brain in normal and diseased conditions. It would be useful for characterizing the property changes of the brain during the developmental processes of certain diseases that affect the WM structures, such as autism (Cook, 1990; Courchesne et al., 2001; Lee et al., 2002) and multiple sclerosis (Graves et al., 1986; Davie et al., 1995). We hope that the obtained information may eventually be useful to the improvement of diagnosis accuracy of such diseases.

This work was partially supported by National Institutes of Health grants NS-37400 and HD 36725 and a Department of Defense grant DAMD17-01-1-0665.

REFERENCES

Blanton, R. E., J. G. Levitt, P. M. Thompson, K. L. Narr, L. Capetillo-Cunliffe, A. Nobel, J. D. Singerman, J. T. McCracken, and A. W. Toga. 2001. Mapping cortical asymmetry and complexity patterns in normal children. *Psychiatry Res.* 107:29–43.

Boult, T. E., and G. Wolberg. 1993. Local image reconstruction and subpixel restoration algorithms. *CVGIP: Graphical Model and Image Processing*. 55:63–77.

Bullmore, E., M. Brammer, I. Harvey, R. Persaud, R. Murray, and M. Ron. 1994. Fractal analysis of the boundary between white matter and cerebral cortex in magnetic resonance images: A controlled study of schizophrenic and manic-depressive patients. *Psychol. Med.* 24:771–781.

Cook, E. H. 1990. Autism: review of neurochemical investigation. *Synapse*. 6:292–308.

Cook, M. J., S. L. Free, M. R. A. Manford, D. R. Fish, S. D. Shorvon, and J. M. Stevens. 1995. Fractal description of cerebral cortical patterns in frontal lobe epilepsy. *Eur. Neurol.* 35:327–335.

Courchesne, E., C. M. Karns, H. R. Davis, R. Ziccardi, R. A. Carper, Z. D. Tigue, H. J. Chisum, P. Moses, K. Pierce, C. Lord, A. J. Lincoln, S. Pizzo, L. Schreibman, R. H. Haas, N. A. Akshoomoff, and R. Y. Courchesne. 2001. Unusual brain growth patterns in early life in patients with autistic disorder: an MRI study. *Neurology*. 57:245–254.

Cross, S. S. 1997. Fractals in pathology. *J. Pathol.* 182:1–8.

Davie, C. A., G. J. Barker, S. Webb, P. S. Tofts, A. J. Thompson, A. E. Harding, W. I. McDonald, and D. H. Miller. 1995. Persistent functional deficit in multiple sclerosis and autosomal dominant cerebellar ataxia is associated with axon loss. *Brain*. 118:1583–1592.

Free, S. L., S. M. Sisodiya, M. J. Cook, D. R. Fish, and S. D. Shorvon. 1996. Three-dimensional fractal analysis of the white matter surface from magnetic resonance images of the human brain. *Cereb. Cortex*. 6:830–836.

Ghez, C., and W. T. Thach. 2000. The cerebellum. *In* Principles of Neural Science, 4th ed. E. R. Kandel, J. H. Schwartz, and T. M. Jessell, editors. McGraw-Hill, New York. 833–835.

Graves, V. B., P. A. Turski, C. M. Strother, L. W. Houston, J. F. Sackett, and L. R. Gentry. 1986. The spectrum of multiple sclerosis lesions using a multiple spin echo pulse sequence and a high field strength. *Acta Radiol. Suppl.* 369:378–381.

Heymans, O., J. Fissette, P. Vico, S. Blacher, D. Masset, and F. Brouers. 2000. Is fractal geometry useful in medicine and biomedical sciences? *Med. Hypotheses*. 54:360–366.

Iftekharuddin, K. M., W. Jia, and R. Marsh. 2000. A fractal analysis approach to identification of tumor in brain MR images. *Eng. Med. Biol. Soc., Proc. of the 22nd Annu. Intl. Conference of the IEEE*. 4:3064–3066.

Kedzia, A., M. Rybaczuk, and R. Andrzejak. 2002. Fractal dimensions of human brain cortex vessels during the fetal period. *Med. Sci. Monit.* 8:MT46–MT51.

Kedzia, A., M. Rybaczuk, and J. Dymecki. 1997. Fractal estimation of the senile brain atrophy. *Folia Morphol. (Praha).* 35:237–240.

Kenkel, N. C., and D. J. Walker. 1996. Fractals in the biological sciences. *Coenoses*. 11:77–100.

Lam, L., S. Lee, and C. Y. Suen. 1992. Thinning methodologies – a comprehensive survey. *IEEE Trans. Patt. Anal. Machine Intell.* 14:869–885.

Lee, M., C. Martin-Ruiz, A. Graham, J. Court, E. Jaros, R. Perry, P. Iversen, M. Bauman, and E. Perry. 2002. Nicotinic receptor abnormalities in the cerebellar cortex in autism. *Brain*. 125:1483–1495.

Losa, G. A. 2000. Fractals 2000 in biology and medicine. *Rivista di Biologia/Biology Forum* 93:295–348.

Mandelbrot, B. B. 1982. The Fractal Geometry of Nature. Freeman, New York.

Pereira, D., C. Zambrano, and M. Martin-Landrove. 2000. Evaluation of malignancy in tumors of the central nervous system using fractal dimension. *Eng. Med. Biol. Soc., 2000. Proc. of the 22nd Annu. Intl. Conference of the IEEE*. 3:1775–1778.

Porter, R., S. Ghosh, G. D. Lange, and T. G. Smith, Jr. 1991. A fractal analysis of pyramidal neurons in mammalian motor cortex. *Neurosci. Lett.* 130:112–116.

Rybaczuk, M., and A. Kedzia. 1996. Fractal analysis of adults cerebellum surface NMR observations. *Folia Morphol. (Praha).* 55:431–433.

Rybaczuk, M., A. Kedzia, and E. Blaszczyk. 1996. Fractal description of cerebellum surface during fetal period. *Folia Morphol. (Praha).* 55: 434–436.

Smith, T. G., Jr., and T. N. Behar. 1994. Comparative fractal analysis of cultured glia derived from optic nerve and brain demonstrate different rates of morphological differentiation. *Brain Res.* 634:181–190.

Smith, T. G., Jr., T. N. Behar, G. D. Lange, W. B. Marks, and W. H. Sheriff, Jr. 1991. A fractal analysis of cultured rat optic nerve glial growth and differentiation. *Neuroscience*. 41:159–166.

Smith, T. G., Jr., K. Brauer, and A. Reichenbach. 1993. Quantitative phylogenetic constancy of cerebellar Purkinje cell morphological complexity. *J. Comp. Neurol.* 331:402–406.

Soltys, Z., M. Ziaja, R. Pawlinski, Z. Setkowicz, and K. Janeczko. 2001. Morphology of reactive microglia in the injured cerebral cortex. Fractal analysis and complementary quantitative methods. *J. Neurosci. Res.* 63:90–97.

Takeda, T., A. Ishikawa, K. Ohtomo, Y. Kobayashi, and T. Matsuoka. 1992. Fractal dimension of dendritic tree of cerebellar Purkinje cell during onto- and phylogenetic development. *Neurosci. Res.* 13:19–31.

Thompson, P. M., C. Schwartz, R. T. Lin, A. A. Khan, and A. W. Toga. 1996. Three-dimensional statistical analysis of sulcal variability in the human brain. *J. Neurosci.* 16:4261–4274.